ELSEVIER

Journal of Photochemistry and Photobiology A: Chemistry 105 (1997) 365–371

Journal of PHOTOCHEMISTRY AND PHOTOBIOLOGY A:CHEMISTRY

The role of conical intersections and excited state reaction paths in photochemical pericyclic reactions

Fernando Bernardi [a,*], Massimo Olivucci [a], Michael A. Robb [b]

[a] *Dipartimento di Chimica "G. Ciamician" dell'Università di Bologna, Via Selmi 2, 40126 Bologna, Italy*

[b] *Department of Chemistry, King's College London, Strand, London WC2R 2LS, UK*

Received 25 September 1996; accepted 13 November 1996

Abstract

In this paper, we discuss the photochemical mechanisms of the following three prototype pericyclic reactions:

1. the electrocyclic ring closure of *cis*-butadiene;
2. the photochemical dimerization of two ethylenes;
3. the photochemical sigmatropic shifts in but-1-ene.

These photochemical reactivity problems have been investigated using an ab initio CAS-SCF approach, followed in some cases by CAS-PT2 calculations.

This study shows that the photochemical mechanisms of these classes of reactions are controlled in each case by a conical intersection between the photochemically relevant excited state and the ground state. In these reactions such conical intersections provide a very efficient means of radiationless deactivation or chemical transformation of the reacting system. © 1997 Elsevier Science S.A.

Keywords: Conical intersections; Excited state reaction paths; Photochemical pericyclic reactions; Van der Lugt–Oosteroff model; Woodward–Hoffmann rules

1. Introduction

Recently, it has been shown that surface crossings play an important role in many photochemical reactions [1,2]. Surface crossings may be divided into conical intersections and intersystem crossings: conical intersections correspond to crossings between states of the same multiplicity (most commonly singlet–singlet), whereas intersystem crossings correspond to crossings between states of different multiplicity (typically singlet–triplet). In suitable conditions, both types of crossing represent very efficient "funnels" for radiationless deactivation or chemical transformation of the system. Recent ab initio CAS-SCF investigations of the potential energy surfaces of the ground and excited states of polyatomic molecules have indicated that low-lying conical intersections occur with previously unsuspected frequency [3]. These intersection points are often located at the end of excited state minimum energy paths (MEPs) starting either in the reactant Franck–Condon (FC) region or in a suitable excited state intermediate well. Such a feature allows a computational, but unambiguous, definition of the excited state reaction coordinate to be made, which is defined by the geometrical deformation undergone by the reactant molecule along the MEP.

The recent computation of excited state reaction coordinates for organic photochemical pericyclic reactions opens up a new perspective in the understanding and interpretation of the currently available theoretical models used for this class of reactions. In this paper, we discuss the role of conical intersections and excited state reaction coordinates in three relevant prototype pericyclic reactions which are all textbook examples for the application of theoretical models. These include the cyclization of butadiene, the cycloaddition of two ethylene molecules and the sigmatropic shift of but-1-ene. All these problems have now been investigated via accurate quantum chemical computations by determining the excited state stationary points (excited state minima, transition states, etc.) and low-lying crossing points and by constructing the reaction MEP. We expect that, similar to thermal (i.e. ground state) reactions, the MEP provides information on the region of the potential energy surface controlling the excited state "average" reactive motion. However, we stress that a MEP and the corresponding reaction coordinate do not provide direct information on the actual reaction dynamics. The

* Corresponding author.

PII S1010-6030(96)04573-X

results obtained are also used to discuss the limitations of the two most popular theoretical models employed to rationalize the photochemical behaviour of pericyclic reactions: the Woodward–Hoffmann [4] and Van der Lugt–Oosteroff [5] models.

2. Theoretical models

In this section, we briefly summarize the main features of the theoretical models most commonly used to rationalize photochemical problems. These models deal with the shape (i.e. the energy profile) of the excited and ground state potential energy surfaces along the reaction coordinate. Therefore, in general, their results can be directly compared with those of MEP construction from ab initio computations. We show below that the major limitations of the two models arise from the fact that in both cases the reaction coordinate is assumed.

2.1. The Woodward–Hoffmann rules

The discovery about 30 years ago by Woodward and Hoffmann of "orbital symmetry conservation" [4] provided a powerful qualitative instrument for discussing thermal and photochemical reactivity. According to these rules, a given reaction can be classified as forbidden or allowed on the basis of orbital correlation diagrams. The classification was also simplified by the derivation of simple selection rules based on the number of π electrons involved in the two reacting systems.

Subsequently, the orbital correlation diagrams were transformed, following the suggestions of Longuet-Higgins and Abrahamson [6], into state correlation diagrams, which have the advantage of showing pictorially the energy profiles along the reaction coordinate. In a state correlation diagram, the fundamental consideration is that states of the same symmetry do not cross, i.e. the result is an avoided crossing, whereas states of different symmetry can cross. For illustrative purposes, a state correlation diagram for the thermally forbidden and photochemically allowed supra–supra cycloaddition of two ethylenes is shown in Fig. 1. The main features of this diagram are as follows:

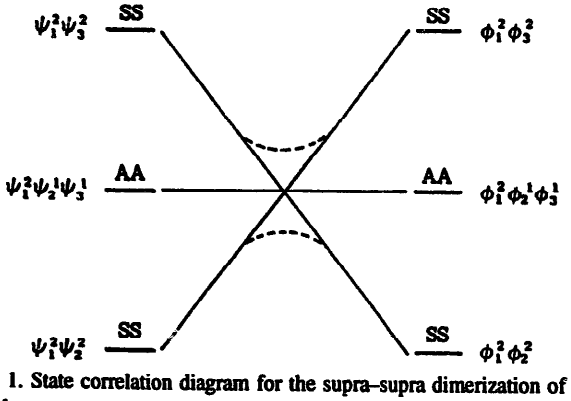

Fig. 1. State correlation diagram for the supra–supra dimerization of two ethylenes.

1. both the ground state configuration of two ethylenes $\Psi_1^2\Psi_2^2$ and the diexcited configuration $\Psi_1^2\Psi_3^2$ are totally symmetric and therefore an avoided crossing results between these two curves;
2. the monoexcited antisymmetric configuration $\Psi_1^2\Psi_2\Psi_3$ correlates with the antisymmetric configuration of the cyclobutane product.

On this basis, the thermal reaction is expected to possess a large barrier (forbidden reaction), whereas the photochemical process will proceed smoothly along the excited state surface (allowed reaction).

The main limitation in the application of this model to photochemical processes is that the Woodward–Hoffmann treatment focuses only on the energetics of the singly excited state, which usually corresponds to the spectroscopic state and does not take into account the possible evolution of different, lower lying, states. Furthermore, the reaction coordinate for the process under investigation must retain the symmetry elements required for the construction of the correlation diagrams all along the reaction path. Despite these limitations, this treatment in many cases predicts the observed stereochemistry as well as the observed reversal of behaviour from thermally difficult to photochemically facile reactions.

The three types of pericyclic reaction discussed in this paper, i.e. the electrocyclic reaction of butadiene, the photodimerization of ethylene and the sigmatropic shift of but-1-ene, are all facile photochemical reactions. As far as the stereochemistry is concerned, for the ring closure of *cis*-butadiene, the Woodward–Hoffmann rules predict the formation of a photoproduct with a rigid disrotatory stereochemistry, whereas in the case of the photocycloaddition of two ethylenes, they predict a facile reaction along a supra–supra reaction path. Similarly, a supra reaction path with retention of configuration at the migrating centre is predicted for the photochemical [1,3]-sigmatropic shift in but-1-ene. As previously pointed out, these rules predict the stereochemical behaviour on the basis of the energy profile of the singly excited spectroscopic state of the system, which is not the lowest excited state in the mechanistically important region. Furthermore, these predictions refer to symmetric reaction coordinates. Below, we try to understand why these rules lead, in many cases, to the observed stereochemical prediction.

2.2. The Van der Lugt–Oosteroff model

About 20 years ago, Van der Lugt and Oosteroff [5] investigated computationally the behaviour of the $1B_2$, $2A_1$ and ground ($1A_1$) states of *cis*-butadiene during ring closure using a four-electron valence bond model. It was shown that, along both the disrotatory and conrotatory coordinates, the $2A_1$ energy profile crosses the $1B_2$ state and evolves into a deep minimum (the so-called "pericyclic" minimum) arising from a $2A_1/1A_1$ avoided crossing. A schematic representation of the results obtained by Van der Lugt–Oosteroff for *cis*-butadiene is shown in Fig. 2. The excited and ground state

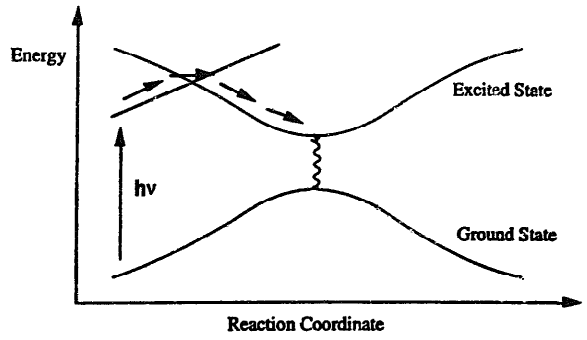

Fig. 2. Schematic representation of the Van der Lugt–Oosteroff diagram for the ring closure of *cis*-butadiene.

energy profiles for both the disrotatory and conrotatory processes are given along assumed symmetric reaction coordinates. The observed disrotatory stereochemical preference along this coordinate was explained on the basis of a smaller excited state to ground state energy gap corresponding to the avoided crossing. In other words, in contrast with the Woodward–Hoffmann treatment, which focuses on the energetics of the $1B_2$ spectroscopic state, the Van der Lugt–Oosteroff model asserts that the rigid stereochemistry is due to the different efficiency of internal conversion from the $2A_1$ to the $1A_1$ state (which depends on the different energy gaps at the disrotatory and conrotatory pericyclic minima).

More recently, similar results have been obtained on the photochemical dimerization of two ethylenes, where again the doubly excited state falls below the singly excited state in the region of the avoided crossing [7].

3. Computational study of photochemical pericyclic reactions

In this section, we summarize the results obtained in an ab initio computational study of the three prototype pericyclic reactions previously considered. In particular, for *cis*-butadiene, we have carried out the computations at the CAS-SCF [8] and CAS-PT2 [9] levels using extended basis sets, whereas for the other two problems, photodimerization and sigmatropic shift, the computations have been carried out only at the CAS-SCF level. In all cases, we used a four electron in four orbital active space. The chosen orbitals comprise all orbitals involved in the description of the bond-breaking/bond-forming processes.

The computation of the MEP and reaction coordinate was performed with the intrinsic reaction coordinate (IRC) method available in the GAUSSIAN 94 package [10]. The search and characterization of the conical intersection points were performed using the method reported in Ref. [11] available in GAUSSIAN 94.

3.1. Photochemistry of butadiene

To rationalize the photochemistry of *cis*-butadiene and, in particular, the corresponding ring-closure electrocyclic reaction, we investigated the full electronic relaxation of the system from the FC region to the ground state surface. For this purpose, we computed the main features of the potential energy surfaces associated with the $2A_1$ covalent state (the HOMO–LUMO doubly excited state) and the $1B_2$ ionic state (the HOMO–LUMO singly excited state) via ab initio quantum chemical computations at a level of theory which includes extended basis sets and dynamic correlation effects (for details, see Ref. [12]). In particular, all the computations on the $2A_1$ state, which include the optimization of all $2A_1$ stationary points, the computation of the MEP and the characterization of the stationary points were carried out at the CAS-SCF level with a DZ+d basis set [13], whereas the corresponding quantities on the $1B_2$ state were carried out at the CAS-SCF level with a basis set which also includes sp-type diffuse functions (DZ+spd). The energetics of the $1B_2$ and $2A_1$ optimized structures were obtained via single-point CAS-PT2F [9] computations with a DZ+spd basis set [13].

The results of this computational study are summarized in Fig. 3 (for details, see Ref. [12]) and show that, on relaxation from the FC region, the photoexcited molecule undergoes a barrierless relaxation, leading ultimately to decay to the $1A_1$ ground state. The following specific results are of interest.

(1) On vertical excitation, the $1B_2$ state is the first excited state. This state has a local equilibrium stationary point of C_s symmetry (C_s-ION). Since no C_2 symmetry stationary point has been located in this region, the shape of the $1B_2$ energy surface favours a disrotatory motion of the two terminal CH_2 groups.

(2) There are two successive intersection points (conical intersections) involved in the relaxation process (see Fig. 3). The first intersection occurs between the spectroscopic $1B_2$ state and the dark $2A_1$ state and is located in the vicinity of the C_s-ION minimum. The second intersection occurs between the $2A_1$ and $1A_1$ states and will be entered after $2A_1$ geometric relaxation.

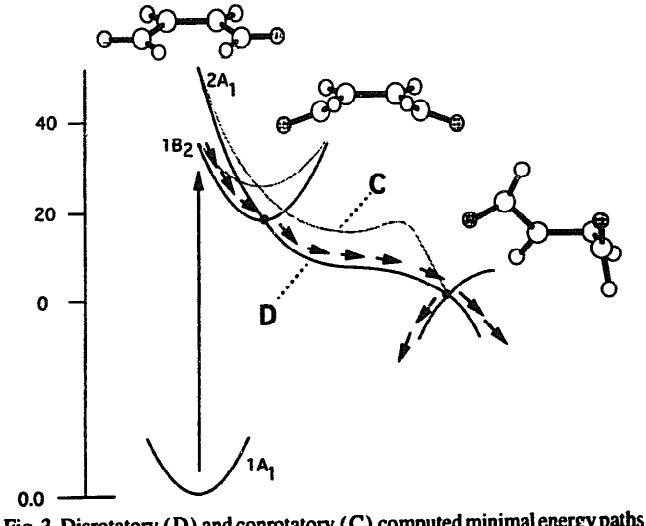

Fig. 3. Disrotatory (D) and conrotatory (C) computed minimal energy paths from the Franck–Condon region to the $2A_1/1A_1$ conical intersection involved in the photochemistry of butadiene.

(3) In the region between the two intersections, the $2A_1$ state becomes the first excited state. At the CAS-SCF level, this state contains two non-planar C_2 and C_s conformers (C_2-MIN and C_s-MIN), with C_s-MIN slightly more stable. Actually, at the CAS-PT2 level, C_s-MIN is not a stationary point, but a point on a flat valley from which the system will evolve towards the $2A_1/1A_1$ conical intersection. However, in addition to this disrotatory path, a conrotatory path exists on the $2A_1$ potential energy surface which will end in the same $2A_1/1A_1$ crossing region. However, while the disrotatory path is barrierless, the conrotatory path has a barrier that is 7 kcal mol^{-1} higher in energy. Thus the structural evolution of the system along the $2A_1$ energy surface will be disrotatory only because the conrotatory path is hindered by a barrier.

A more rigorous rationalization of the disrotatory stereochemical preference can only be obtained by taking into account the geometrical relaxation dynamics of the photoexcited reactant. Our potential energy surfaces suggest that, after photoexcitation to the $1B_2$ state, the system will enter the $2A_1$ potential energy surface with a large velocity component along the disrotatory coordinate, but with no component along the conrotatory coordinate. Thus the only way to populate the $2A_1$ conrotatory path is to redistribute approximately 15 kcal mol^{-1} of excess kinetic energy (see energy diagram in Fig. 3) on the disrotatory mode between the other vibrational degrees of freedom of the molecule. However, since the $2A_1$ disrotatory path is barrierless and the conrotatory path is 7 kcal mol^{-1} higher in energy, the conical intersection is expected to be reached along a disrotatory path on a timescale faster than the energy redistribution.

(4) Direct irradiation of *cis*-butadiene yields a mixture of cis–trans isomerization and cyclization products [14,15]. These experimental results are well rationalized by the computed structure of the $2A_1/1A_1$ conical intersection (see Fig. 4) and by the computed shape of the disrotatory reaction path which involves simultaneous twisting motion about the central C–C bond and asynchronous disrotatory rotation of the two terminal methylenes. The computational results suggest that the electronic structure of the conical intersection is

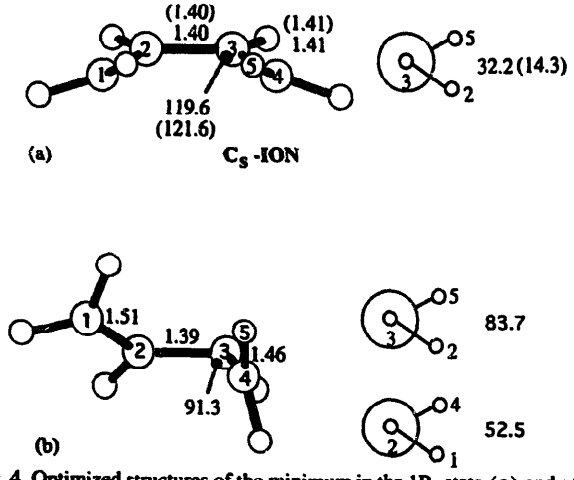

Fig. 4. Optimized structures of the minimum in the $1B_2$ state (a) and of the $2A_1/1A_1$ conical intersection (b).

that of a quasi-tetraradical in which four unpaired electrons are almost isolated on the four carbon atoms of the butadiene framework. The recoupling process starts at the conical intersection and will be responsible for the simultaneous formation of the various photoproducts. The various recoupling pathways will be differently populated according to the particular geometric structure of the conical intersection point.

(5) While the ring-closure reaction of butadiene is stereospecific, the reverse reaction, i.e. the ring opening of cyclobutene, shows a lack of stereochemistry [16]. This experimental observation can be explained by assuming that the cyclobutene ring opens on the $1B_2$ state. In this way, the cyclobutene photolysis will yield $1B_2$ *cis*-butadiene which decays to the $2A_1$ state following the disrotatory path illustrated in Fig. 3. The final photoproducts of the reverse reaction must originate via decay at the same $2A_1/1A_1$ conical intersection and will follow the relaxation pathway previously discussed. It is obvious from the structure of the conical intersection that decay at this point involves cis–trans double-bond isomerization so that the production of a stereospecific (disrotatory) ring-opening butadiene is impossible.

In agreement with the present computational results, both the Woodward–Hoffmann and Van der Lugt–Oosteroff theoretical models predict the ring-closure reaction to evolve with a rigid disrotatory, as opposed to conrotatory, stereochemistry. Since the Woodward–Hoffmann rules only predict favourable disrotatory energetics on the spectroscopic state, it is not obvious why they work. Of course, the calculation shows that, in this case, the full relaxation pathway from the FC region to the ground state surface always corresponds to the region with disrotatory character. However, this can hardly be argued to be general.

Another interesting refinement to the standard interpretation of the Woodward–Hoffmann rules suggested by our results for the $1B_2$ state regards the shapes of the allowed (disrotatory) and forbidden (conrotatory) energy profiles. The theory predicts a large barrier along the forbidden path and a barrierless allowed path. The computed allowed energy profile corresponds to a real MEP and is indeed barrierless. However, the symmetry constrained conrotatory (i.e. forbidden) path is also barrierless (see Fig. 3). The real difference between the allowed and forbidden paths is in the energy slope and, most important, in the actual shape of the potential energy surface along the allowed and forbidden coordinates. In fact, the forbidden coordinate not only has a less sloped energy profile, but runs along a ridge of the potential energy surface and thus does not correspond to a real MEP on the spectroscopic potential energy surface.

The differences between the results obtained by Van der Lugt–Oosteroff and the ab initio results summarized above are also significant and are mainly caused by the differences in the reaction coordinate along the low-lying $2A_1$ excited state. In fact, the Van der Lugt–Oosteroff computations assume that the excited state reaction path closely resembles the symmetry adapted pathway found for the ground state ring closure. Use of this path leads to the avoided crossing,

while the use of the proper optimized reaction path leads to the conical intersection as specified in part (4) above. While this result can be seen as a refinement of the Van der Lugt–Oosteroff theory, the actual interpretation of the stereochemical selectivity in the two cases changes completely. In the Van der Lugt–Oosteroff model, this is based on energy gaps. In contrast our computations suggest that the selectivity can be due to the most favourable energetics along a disrotatory path, which is barrierless on the $2A_1$ surface, while the forbidden conrotatory path is impaired by an energy barrier. On the other hand, the decay rates are expected to be very similar at the two decay points. In fact, in general, both pathways lead to a conical intersection (which is the same in the case of *cis*-butadiene): since decay at a conical intersection is always very fast, there must not be any difference in the decay rates at these points.

3.2. Photochemical cycloaddition of two ethylenes

The results reported in the previous section show the importance of the doubly excited covalent potential energy surface. In the other two prototype pericyclic reactions investigated, we have limited our computational study only to the potential energy surface associated with the covalent state. The results of the computational study for the singlet photochemical cycloaddition of two ethylenes are illustrated in Fig. 5 (for details, see Ref. [17]). The computations in this case have been carried out at the CAS-SCF/4-31G level [8].

The predictions of the Woodward–Hoffmann rules for this photochemical reaction are based on a supra–supra concerted approach on the ionic singly excited state. In this case, the Woodward–Hoffmann rules make the prediction that this photochemical reaction occurs easily via a supra–supra approach, yielding the photoproduct in an excited state (see Fig. 1). This is in contrast with the experimental [18] and computational (see below) evidence. Also, the Van der Lugt–Oosteroff model assumes a supra–supra path as the reaction coordinate, and along this path the $S_1 \rightarrow S_0$ decay occurs at an avoided crossing between the doubly excited state S_1 and the ground state S_0, which produces the pericyclic minimum in the excited state (A in Fig. 5) and the pericyclic maximum in the ground state (A′ in Fig. 5) surface.

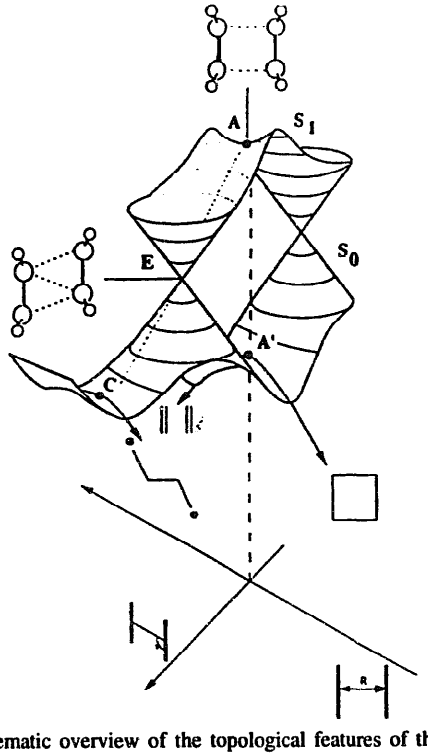

Fig. 5. Schematic overview of the topological features of the S_1 and S_0 potential energy surfaces for the singlet photocycloaddition of two ethylenes.

This decay mechanism is not consistent with our MC-SCF/4-31G computations. While the full geometry optimization carried out in the region of the avoided crossing confirms that A and A′ are both stationary points, vibrational frequency computations show that A is a transition state and A′ is a second-order saddle point. Since the energy difference between A and A′ is larger than 50 kcal mol^{-1} and A is a transition structure, an excited state relaxation pathway cannot pass through A. The search for a true S_1 minimum carried out at the same level of theory leads to two lowest energy regions of the excited state surface located far away from the supra–supra reaction coordinate. These regions are centred on two singularities (i.e. cusps) corresponding to upper halves of two identical conical intersections where the excited and ground state surfaces are degenerate (E in Fig. 5). These intersections and surrounding regions are located at the bottom of the two valleys separated by the transition state A and correspond to the absolute minima of the S_1 excited state surface.

Our computations suggest a mechanistic scheme (see Fig. 5) which differs from the previously proposed mechanism and, in particular, from the Van der Lugt–Oosteroff view. In this scheme, the photoreacting system falls down the funnels created by the conical intersections and passes almost directly to the ground state via a fast internal conversion. No excited state intermediate (i.e. no pericyclic minimum) is thus generated on this state. During the barrierless decay, the stereochemistry of the olefin moiety is retained because the excited state lifetime is very short due to the presence of a conical intersection and all along the reaction coordinate and at the conical intersection the system has a well-defined and rigid molecular structure. This structure (which has C_{2h} symmetry) is shown in Fig. 6.

The C_{2h} conical intersection arises from the crossing of the doubly excited covalent state with the ground state, with the

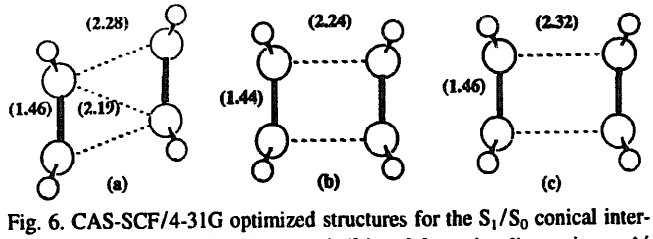

Fig. 6. CAS-SCF/4-31G optimized structures for the S_1/S_0 conical intersection (a), the pericyclic minimum A (b) and the pericyclic maximum A′ (c).

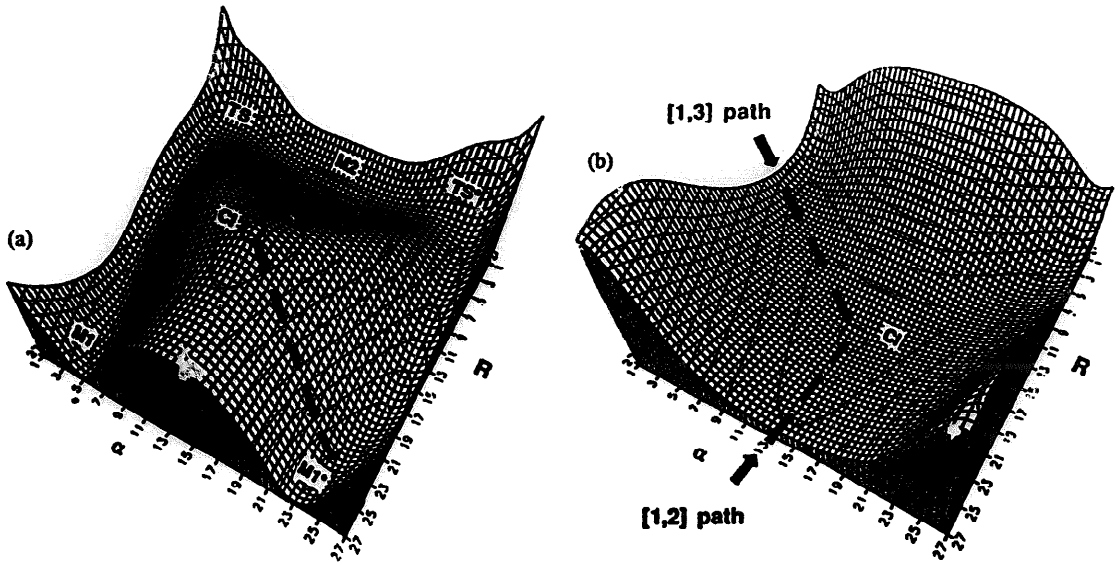

Fig. 7. Ground state (a) and excited state (b) potential energy surfaces for the [1,2]- and [1,3]-sigmatropic shifts in but-1-ene. The coordinates are R (the distance between the central C of the allyl fragment and the C of the CH_3 migrating fragment) and α (the angle between the R axis and the C–C bond axis of the allyl fragment).

two interacting olefinic fragments rigidly bound in a rigid rhomboid structure. As a consequence (in a substituted π system), the system will decay to the ground state and form a four-membered ring photoproduct without loss of stereochemistry. Thus, remarkably, the S_1 reaction path for the photocycloaddition process appears to be very different in both geometrical structure and energetics from the proposed D_{2h} supra–supra reaction path. According to our computations, the latter path seems to define a ridge rather than an energetically stable valley on the excited state surface. The computed reaction path is also very different from the cycloaddition reaction pathway found on the ground state surface. In fact, according to this pathway, the thermal cycloaddition involves the generation of diradical species which are very different from the C_{2h} conical intersection structure seen above.

3.3. Photochemical sigmatropic rearrangement of but-1-ene

Sigmatropic shifts represent another important class of pericyclic reaction. Of particular interest are the photochemical [1,3]- and [1,2]-sigmatropic shift reactions, which are relatively common in the singlet excited state. To obtain information on the mechanisms of these photochemical reactions, we carried out a theoretical investigation on the ground and first excited states of the model system but-1-ene, where the sigmatropic process involves the migration of a CH_3 group on an allyl fragment and can produce either a [1,3]- or [1,2]-sigmatropic shift.

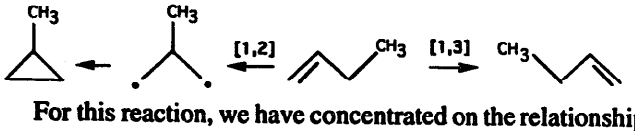

For this reaction, we have concentrated on the relationship between the ground state and the covalent singlet excited state, which, as previously shown, is the lowest excited state. The details of the CAS-SCF/4-31G results for the model but-1-ene system are given in Ref. [19].

The results obtained for both the ground and excited states are pictorially illustrated in Fig. 7, where two-dimensional cross-sections of both the ground and excited state potential energy surfaces are shown. We discuss first the results obtained for the excited state. There appears to be no minimum (in the usual meaning of the word) in the excited state. Rather, all attempts to optimize a minimum on the singlet excited state potential energy surface converge to a conical intersection point where the ground and excited states are degenerate. The structure assumed by the reacting system at the optimized conical intersection point is shown in Fig. 8. The results obtained for the ground state are summarized in Fig. 7, where M1 and M1* are the reactant and the (degenerate) product respectively of the [1,3]-shift reaction and TS, TS* and M2 are the transition states and diradical product associated with the [1,2]-shift process.

The occurrence of a conical intersection implies that the return to the ground state must be fully efficient. Thus there

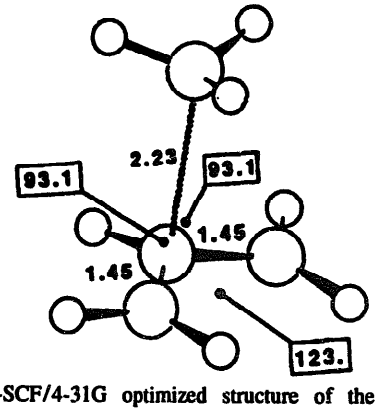

Fig. 8. CAS-SCF/4-31G optimized structure of the S_1/S_0 conical intersection.

is no bottleneck due to a short-lived intermediate which would correspond to a minimum on the excited state surface at an avoided crossing. Consequently, the stereochemistry is preserved and the process concerted. The IRC computations demonstrate the existence of two "channels" on the excited state surface which simply "continue" on the ground state surface. One of these channels leads to a [1,2]-sigmatropic shift and the other to a [1,3]-sigmatropic shift. The proposed mechanism is consistent with experimental observations, where both [1,2]- and [1,3]-shift products are observed and where the migrating group moves according to a supra process with retention of configuration of the migrating group. This behaviour is also in agreement with the Woodward–Hoffmann selection rules for a concerted [1,3]-sigmatropic shift. However, as pointed out by other workers [20], the same rules make no prediction that [1,3]- and [1,2]-shifts will be competitive in the same system with the same stereochemistry, as rationalized by the conical intersection mechanism presented in this paper.

4. Conclusions

The computational study of the prototype photochemical pericyclic reactions presented in this paper shows that the photochemical mechanism of this class of reactions is controlled by reaction coordinates which access conical intersections between the photochemically relevant excited states and the ground state. This finding indicates that the previous theoretical models need to be considerably refined. Furthermore, MEP computations indicate that the excited state reaction coordinate does not retain symmetry. The present computational results show that each type of pericyclic reaction has its own conical intersection structure varying from rhomboid to more complex open-chain structures as previously discussed. The conical intersections, which represent the "photochemical funnel" introduced by Zimmerman [21] and Michl [22], provide a fully efficient means for the radiationless deactivation or chemical transformation of the system. Thus, as observed in the case of *cis*-butadiene photochemistry, when both the "allowed" and "forbidden" excited state reaction coordinates lead to a conical intersection point, the selectivity must be controlled by the existence and energetics of the corresponding excited state reaction paths.

References

[1] M. Klessinger, Angew. Chem. Int. Ed. Engl. 34 (1995) 549.

[2] M. Klessinger, J. Michl, Excited States and Photochemistry of Organic Molecules, VCH, New York, 1995.

[3] I.J. Palmer, I.N. Ragazos, F. Bernardi, M. Olivucci, M.A. Robb, J. Am. Chem. Soc. 115 (1993) 673. P. Celani, S. Ottani, M. Olivucci, F. Bernardi, M.A. Robb, J. Am. Chem. Soc. 116 (1994) 10 141. P. Celani, M. Garavelli, S. Ottani, F. Bernardi, M.A. Robb, M. Olivucci, J. Am. Chem. Soc. 117 (1995) 11 584. I.J. Palmer, I.N. Ragazos, F. Bernardi, M. Olivucci, M.A. Robb, J. Am. Chem. Soc. 116 (1994) 2121. M. Reguero, M. Olivucci, F. Bernardi, M.A. Robb, J. Am. Chem. Soc. 116 (1994) 2103, and references cited therein. S. Wilsey, M.J. Bearpark, F. Bernardi, M. Olivucci, M.A. Robb, J. Am. Chem. Soc. 118 (1996) 176. N. Yamamoto, F. Bernardi, A. Bottoni, M. Olivucci, M.A. Robb, S. Wilsey, J. Am. Chem. Soc. 116 (1994) 2064, and references cited therein. S. Wilsey, M.J. Bearpark, F. Bernardi, M. Olivucci, M.A. Robb, J. Am. Chem. Soc., 118 (1996) 4469. M.M.J. Bearpark, F. Bernardi, S. Cliffort, M. Olivucci, M.A. Robb, B.R. Smith, T. Vreven, J. Am. Chem. Soc. 118 (1996) 169.

[4] R.B. Woodward, R. Hoffmann, Angew. Chem. Int. Ed. Engl. 8 (1969) 781.

[5] W.T.A.M. Van der Lugt, L.J. Oosteroff, J. Am. Chem. Soc. 91 (1969) 6042.

[6] H.C. Longuet-Higgins, E.W. Abrahamson, J. Am. Chem. Soc. 87 (1965) 2045.

[7] E. Kassab, E.M. Evleth, J.J. Dannenberg, J.C. Rayez, Chem. Phys. 52 (1980) 151.

[8] The CAS-SCF program we used is implemented in: M.J. Frisch, G.W. Trucks, M. Head-Gordon, P.M.W. Gill, M.W. Wong, J.B. Foresman, B.G. Johnson, H.B. Schlegel, M.A. Robb, E.S. Replogle, R. Gomperts, J.L. Andres, K. Raghavachari, J.S. Binkley, C. Gonzalez, R.L. Martin, D.J. Fox, D.J. Defrees, J. Baker, J.J.P. Stewart, J.A. Pople, GAUSSIAN 92, Revision B, Gaussian, Inc., Pittsburgh, PA, 1992.

[9] K. Andersson, M.R.A. Blomberg, M. Fulscher, V. Kello, R. Lindth, P.Å. Malmqvist, J. Noga, J. Olsen, B.O. Roos, A.J. Sadlej, P.E.M. Siegbahn, M. Urban, P.O. Widmark, MOLCAS, Version 2, University of Lund, Sweden, 1991; P.O. Widmark, IBM, Sweden, 1991.

[10] M.J. Frisch, G.W. Trucks, H.B. Schlegel, P.M.W. Gill, B.G. Johnson, M.A. Robb, J.R. Cheeseman, T. Keith, G.A. Petersson, J.A. Montgomery, K. Raghavachari, M.A. Al-Laham, V.G. Zakrzewski, J.V. Ortiz, J.B. Foresman, J. Cioslowski, B.B. Stefanov, A. Nanayakkara, M. Challacombe, C.Y. Peng, P.Y. Ayala, W. Chen, M.W. Wong, J.L. Andres, E.S. Replogle, R. Gomperts, R.L. Martin, D.J. Fox, J.S. Binkley, D.J. Defrees, J. Baker, J.P. Stewart, M. Head-Gordon, C. Gonzalez, J.A. Pople, GAUSSIAN 94, Revision C.3, Gaussian, Inc., Pittsburgh, PA, 1995.

[11] I.N. Ragazos, M.A. Robb, F. Bernardi, M. Olivucci, Chem. Phys. Lett. 197 (1992) 217. M.J. Bearpark, M.A. Robb, H.B. Schlegel, Chem. Phys. Lett. 223 (1994) 269.

[12] P. Celani, F. Bernardi, M. Olivucci, M.A. Robb, J. Chem. Phys. 102 (1995) 5733.

[13] The DZ, DZ+d and DZ+spd basis sets used in this work correspond to the standard Gaussian 94 basis sets: M.J. Frisch, G.W. Trucks, H.B. Schlegel, P.M.W. Gill, B.G. Johnson, M.A. Robb, J.R. Cheeseman, T. Keith, G.A. Petersson, J.A. Montgomery, K. Raghavachari, M.A. Al-Laham, V.G. Zakrzewski, J.V. Ortiz, J.B. Foresman, J. Cioslowski, B.B. Stefanov, A. Nanayakkara, M. Challacombe, C.Y. Peng, P.Y. Ayala, W. Chen, M.W. Wong, J.L. Andres, E.S. Replogle, R. Gomperts, R.L. Martin, D.J. Fox, J.S. Binkley, D.J. Defrees, J. Baker, J.P. Stewart, M. Head-Gordon, C. Gonzalez, J.A. Pople, GAUSSIAN 94, Revision C.3, Gaussian, Inc., Pittsburgh, PA, 1995.

[14] W.J. Leigh, Can. J. Chem. 71 (1993) 147.

[15] M. Squillacote, T.C. Sample, J. Am. Chem. Soc. 112 (1990) 5546.

[16] W.J. Leigh, K. Zeng, J. Am. Chem. Soc. 113 (1991) 2163.

[17] F. Bernardi, S. De, M. Olivucci, M.A. Robb, J. Am. Chem. Soc. 112 (1990) 1737.

[18] A. Gilbert, J. Baggott, Essentials of Molecular Photochemistry, Blackwell Scientific Publications, Oxford, 1991.

[19] F. Bernardi, S. De, M. Olivucci, M.A. Robb, G. Tonachini, J. Am. Chem. Soc. 114 (1992) 5805.

[20] E.C. Sanford, G.S. Hammond, J. Am. Chem. Soc. 92 (1970) 3497.

[21] H.E. Zimmerman, J. Am. Chem. Soc. 88 (1966) 1566.

[22] J. Michl, J. Mol. Photochem. (1972) 243.